Magnetic Möbius stripe without frustration: Noncollinear metastable states

S. Castillo-Sepúlveda, R. A. Escobar, and D. Altbir
Departamento de Física, CEDENNA, Universidad de Santiago de Chile, USACH, Avenida Ecuador 3493, Santiago, Chile

M. Krizanac and E. Y. Vedmedenko
Physics Department, University of Hamburg, Jungiusstraße 11, Hamburg, Germany
(Received 24 June 2016; published 19 July 2017)

The recently introduced area of topological magnetism searches for equilibrium structures stabilized by a combination of interactions and specific boundary conditions. Until now, the internal energy of open magnetic chains has been explored. Here, we study the energy landscape of closed magnetic chains with on-site anisotropy coupled with antiferromagnetic exchange and dipolar interactions analytically and numerically. We show that there are many stable stationary states in closed geometries. These states correspond to the noncollinear spin spirals for vanishing anisotropy or to kink solitons for high magnetic anisotropy. Particularly, the noncollinear Möbius magnetic state can be stabilized at finite temperatures in nonfrustrated rings or other closed shapes with an even number of sites without the Dzyaloshinskii-Moriya interaction. We identify the described configurations with the stable stationary states, which appear due to the finite length of a ring.

DOI: 10.1103/PhysRevB.96.024426

I. INTRODUCTION

In electronics one uses electric fields for the transmission and processing of information. In spintronics both electric and magnetic fields are utilized. The information processing can also be achieved without any global fields or currents just using the combination of spin degree of freedom subjected to internal interactions such as exchange, Ruderman-Kittel-Kasuya-Yosida (RKKY), or long-range dipolar interactions with specific boundary conditions [1–3]. The combination of interactions with boundary conditions is interesting not only for practical reasons but also from the theoretical point of view as it gives rise to the direction of topological magnetism [1,4]. Topological magnetism is the successor of investigations on metastable magnetic configurations [5,6] and searches for conditions of stabilization of exotic magnetic states. Until now linear classical [1,7,8] and quantum [9] spin chains have been studied. One of the well-known exotic magnetic states is the Möbius magnetic structure. This configuration is also known as the antiferromagnetic spin spiral (AFSS). This structure corresponds to the lowest energy state [10] for antiferromagnetic chains (see Fig. 1).

Nowadays, in addition to linear chains a variety of one-dimensional magnetic ring structures with different anisotropy axes can be experimentally produced. This list includes atomic spin ensembles [10–12], magnetic nanoarrays [13–15], and molecular ring structures [16–18], among others. Here, we are querying which metastable solutions are possible in closed geometries and how the on-site anisotropy influences these metastable states. Another important subject is the role of the free energy in the stabilization of those excited states.

For these purposes, in this paper we study stationary equilibrium magnetic configurations of rings formed by effective magnetic moments coupled via short- or long-range interactions. The main objective of our work is to identify which kind of magnetic states different from the collinear ground states can be stabilized in closed geometries. Particularly interesting appear antiferromagnetic rings. Rings comprising an odd number of magnetic moments became a prototype of frustrated magnetism, because the incommensurability of the odd number of sites with antiferromagnetic interactions leads to the formation of magnetic spirals. By means of analytical and Monte Carlo (MC) simulations the effect of changing the number of atoms, the anisotropy constant, and the dipolar energy on the stable configurations is explored. It has been found that there are many stable stationary states in closed geometries. These states correspond to noncollinear metastable spin spirals for vanishing anisotropy or to magnetic solitons for high magnetic anisotropy. Particularly, the Möbius magnetic configuration can be achieved not only in chains with an odd number of magnetic moments as initially predicted, but can also be stabilized in closed chains with an even number of spins. The lifetimes of such equilibrium noncollinear metastable states in chains with dipolar interactions is larger or comparable with the observation time in typical experiments.

II. ANALYTICAL CALCULATION OF THE GROUND STATE

We use an atomistic Heisenberg-like model in our calculations. Particularly, the considered rings are composed of a circular line of Fe atoms a distance $a = 2.8$ Å apart. Each atom is represented by a Heisenberg magnetic moment $\vec{\mu}_i = \mu_s \vec{S}_i$, with $\mu_s = 2.2\mu_B$ mimicking a typical atomic or molecular chain, and $\vec{S}_i$ the unit and dimensionless vector parallel to $\vec{\mu}_i$. The magnetic moments can be coupled by dipolar and exchange interactions and experience an anisotropic field, as described by the following Hamiltonian:

$$E = \frac{1}{2}\sum_{i\neq j}(DE_{ij} - J_{ij}\vec{S}_i \cdot \vec{S}_j) - K\sum_i(\vec{S}_i \cdot \hat{z})^2, \qquad (1)$$

where E_{ij} is the dipolar energy given by

$$E_{ij} = \omega\frac{\vec{S}_i \cdot \vec{S}_j - 3(\hat{n}_{ij} \cdot \vec{S}_i)(\hat{n}_{ij} \cdot \vec{S}_j)}{r_{ij}^3}, \qquad (2)$$

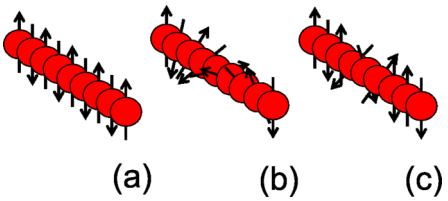

FIG. 1. (a) AFM configuration, (b) AFSS Möbius-like configuration, and (c) KS configuration.

with $r_{ij} = |\vec{r}_i - \vec{r}_j|$, $\hat{n}_{ij} = (\vec{r}_j - \vec{r}_i)/r_{ij}$, and $\omega = \mu_0 \mu_s^2/4\pi$, with μ_0 the magnetic permeability in the vacuum. In these expressions D is a constant that allows us to turn on or off the dipolar interaction by taking the values 1 or 0, and is dimensionless. The exchange interaction constant J_{ij} is equal to J for nearest-neighbor moments and zero otherwise. K is the anisotropy constant that represents the direction of the easy axis. $K > 0$ describes an easy axis along $\hat{z}$, and $K < 0$ is used when the easy plane is perpendicular to $\hat{z}$.

For the sake of clarity we start our study with analytical calculations of the internal energy of a ring of Heisenberg spins subject to the on-site magnetic anisotropy and coupled by an antiferromagnetic exchange interaction. The ground state of such chain or ring with even number of particles corresponds to the collinear antiparallel alignment of neighboring moments. This ideal antiferromagnetic (AFM) configuration is not possible in rings consisting of an odd number of moments. In this case, the AFSS state appears, with the two ends of a chain are antiparallel, while all other spins are forced to rotate in order to satisfy these boundary conditions. On the other hand, also the so-called kink solitons have been found experimentally in layered systems [19]. These structures differ from the Möbius configuration by the width of the spiral structure and consist of ideal antiferromagnetic domains with narrow kinklike solitons (KS) in between (see Fig. 1). The kink solitons are of high technological importance as they can be used as bits of information in magnetic storage and logical devices [19–21].

In our analytical investigations we calculate energies of the pure AFM state, broad AFSS, and two AFM domains with a KS in between. For this purpose the AFM and the AFSS magnetic configurations are mixed with an antiferromagnetic state with kink solitons. If we consider a closed chain with N magnetic moments, a KS contains M magnetics moments, with $M < N$. In this way, the AFM region is formed by $(N - M)$ magnetics moments. The internal energy of the ring is then given by contributions from both regions: the kink solitons and the antiferromagnetic domains.

First we study the situation with $M = N$; that is, the AFSS is homogeneous and as wide as the ring itself. Magnetization of such a spiral can be described as

$$\vec{S}\left(i, \Delta\theta_k^{(N)}\right) = \sin\left[(i-1)\Delta\theta_k^{(N)}\right]\hat{x} + \cos\left[(i-1)\Delta\theta_k^{(N)}\right]\hat{z}, \tag{3}$$

where i defines the coordinate along the ring and $\Delta\theta_k^{(N)} = 2\pi k/N$ is the angle between two neighboring moments as shown in the Appendix. Figure 2 illustrates the internal energy E for chains with even and odd numbers of sites

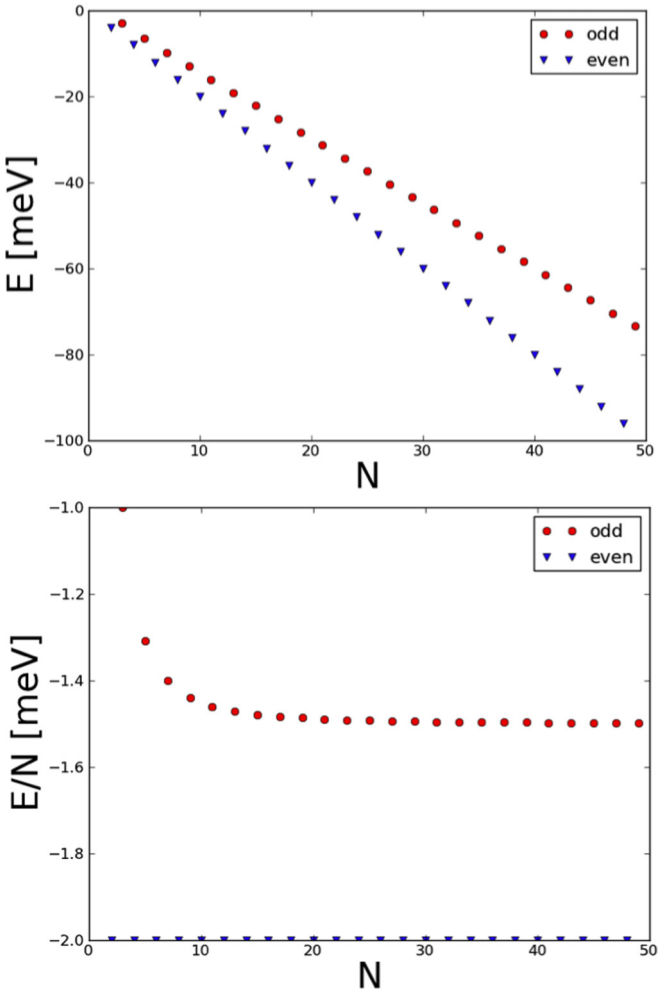

FIG. 2. (a) Internal energy of a pure AFSS state for even and odd number of magnetic moments N when $K = -J = 1$ meV. When N is even, the AFSS state is identical to the AFM state. (b) Internal energy normalized by N for the same parameters used in (a). We observed that if N increases, the difference $|E_N/N - E_{N+1}/(N+1)|$ converges to 0.502 meV. We see that the AFSS state for odd number of magnetic moments is not the minimum of the energy.

acquiring these broad solitons (see the Appendix). Figure 2(b) illustrates the convergence of the normalized internal energy when $N > 10$. In this range, the difference of the energies of rings with N and $N + 1$ magnetic moments is given by $|E_N/N - E_{N+1}/(N+1)| = 0.502$ meV. Explicitly, when N is even, the minimal energy corresponds to

$$E = -N(K - J), \tag{4}$$

and for N odd, the minimal energy is

$$E = JN\cos(\pi/N) - K\sum_{i=1}^{N}\cos^2[(i-1)\pi/N]. \tag{5}$$

These two expressions lead to the following conclusions. For low anisotropies ($|K| < |J|$) and $D = 0$, the lowest energy state for even N corresponds to an AFM configuration, which is equivalent to an AFSS with $\Delta\theta = \pi$. Any other kind of AFSS possess higher energy. The total energy of an AFSS in a chain with an odd number of sites is always larger than

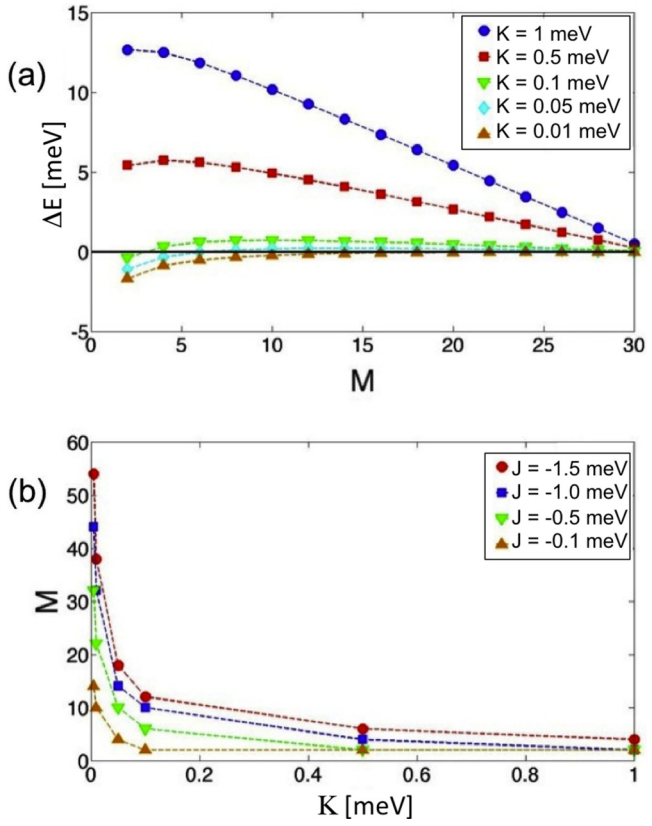

FIG. 3. (a) Difference between the internal energies of the AFSS and KS states for $N = 31$, $J = -1$ meV, and different values for K. $\Delta E > 0$ indicates that a knot is present. (b) Size of a kink soliton (knot) as function of the anisotropy for $N = 31$.

that of the closest chain with an even number of moments $N_{\text{even}} = N_{\text{odd}} \pm 1$. The larger the length of those two chains, the more pronounced the total energy difference despite the almost identical length (± 1) as seen in Fig. 2. This effect occurs due to the frustration inherent to odd chains. Longer chains exhibit a higher degree of frustration, so their energy is larger as compared to a chain with an even number of spins. It becomes also clear from our calculations in the Appendix that the internal energy for chains with odd N can be reduced with replacement of a broad soliton by a combination of an antiferromagnetic domain with a narrow KS.

To make the last statement more apparent we calculate the difference ΔE_N between the energy of an AFSS state $[E(AFSS_M^N)]$ and a KS state $[E(KS_N)]$ as a function of kink soliton length M. The explicit expression is $\Delta E_N = E(AFSS_M^N) - E(KS_N) = \mathcal{K}(N) - \mathcal{K}(M)$, with

$$\mathcal{K}(x) = -Jx[1 - \cos(\pi/x)] - K\sum_{i=1}^{x}\cos^2[(i-1)\pi/x] + Kx. \quad (6)$$

We find that the total energy of a kink-soliton solution is still slightly larger than the energy obtained for chains with an even number of sites of similar length (± 1). However, KSs of a certain width indeed minimize the energy. Figure 3(a) depicts ΔE_N for $N = 31$, $J = -1.0$ meV, and different values of K, while Fig. 3(b) illustrates the size of the KS (knot) that minimizes the energy as a function of J. If $\Delta E_N < 0$ the lowest energy state is the AFSS, while if $\Delta E_N > 0$, the lower energy corresponds to a KS state. We observe that larger anisotropy values K are associated with smaller kink solitons. This finding is in good agreement with experiments: the larger the anisotropy, the narrower the antiferromagnetic domains walls typically are. Hence, from the point of view of internal energy the ground state of rings with an even number of constituents is an AFM configuration, while that of rings consisting of an odd number of magnetic moments corresponds to the KS configurations. Herewith we have shown that in closed rings with an odd number of particles the KS is the stable magnetic configuration, while the soliton width depends on material parameters. The ground state of closed rings with an even number of spins is an ideal AFM configuration.

III. ANALYTICAL CALCULATION OF THE LOWEST EXCITED STATES

In the next step we analyze the lowest excited configurations of rings with an even number of spins as well as their free energy. Since spin spirals are exact solutions of the Heisenberg exchange model for periodic systems, the lowest excited, metastable configurations of such structures can be searched in the phase space of noncollinear spin spirals [22]. First we restrict our calculations considering an anisotropy axis parallel to the ring's axis. For that purpose, AFSS magnetization configurations with the wave vector $\Delta\theta$ have been chosen and the corresponding internal energy $E(\Delta\theta)$ has been calculated analytically or numerically. Surprisingly, in addition to the global energy minima corresponding to configurations with all spins parallel or antiparallel to the z axis described in the previous section, the anisotropy energy of a chain with pairwise spin interactions shows additional, local energy minima corresponding to the noncollinear states. The number of those local energy minima is proportional to the number of spins N in a chain or the closed structure.

An example of an internal energy landscape is given in Fig. 4(a) for a chain consisting of four magnetic moments subject to the uniaxial anisotropy and the exchange interaction $J < 0$. This example concerns the case of an AFSS with the angle $\Delta\theta \subset [0,\pi]$ between nearest-neighboring spins. Only the angle between the first and the last spins in a chain can differ from $\Delta\theta$ if $N\Delta\theta/\pi$ is not integer. The abscissa gives the polar spherical angle θ_1 of the first spin with respect to the z axis. The spiral is two-dimensional, i.e., the four spins have the following S_z components: $\cos(\theta_1)$, $\cos(\theta_1 + \Delta\theta)$, $\cos(\theta_1 + 2\Delta\theta)$, and $\cos(\theta_1 + 3\Delta\theta)$. In this, simplest possible case, the three nontrivial periodic configurations correspond to $\Delta\theta = \pi/4$, $\pi/2$, $3\pi/4$ defining π, 2π, 3π magnetization rotations along a chain, respectively. For $|K| \gg |J|$, these configurations correspond to the band of low-energy saddle points as seen in Fig. 4(a). Additionally, there are 12 local energy minima [blue in Fig. 4(a)]. Six of them (dark blue) correspond to collinear ground states, but the six other (light blue) to noncollinear metastable configurations with $\Delta\theta = \pi/3$ or $2\pi/3$. Hence, already a very short chain with an even number of magnetic moments at zero temperature can be frozen in a noncollinear state if the anisotropy is high enough. Inclusion of the dipolar coupling enhances this effect.

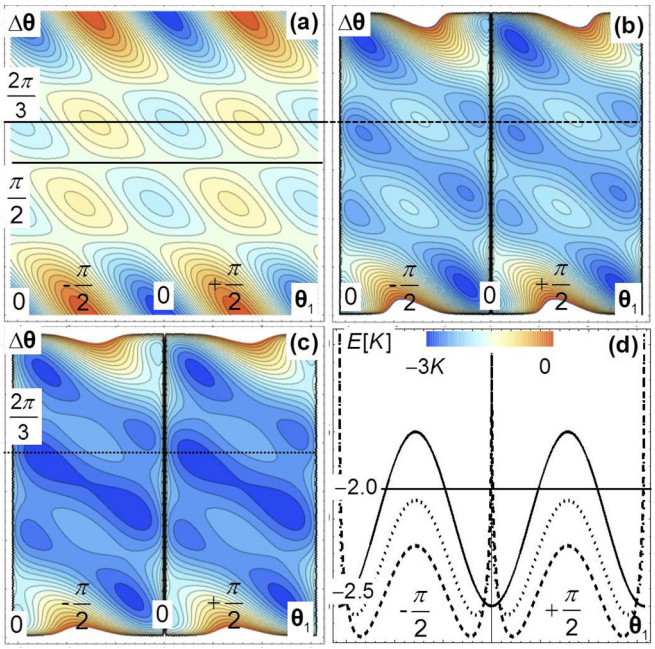

FIG. 4. Analytical calculation of the internal (a) and Gibbs free energy (b)–(d) of the four effective magnetic moments coupled by nearest-neighbor exchange interaction J and subject to uniaxial anisotropy K for $|K| \gg |J|$. $\Delta\theta$ is the angle between the nearest-neighboring spins, while θ_1 is the absolute polar spherical angle of the first spin. The color scheme goes from dark blue (dark gray) for low energies to light (light gray) for high energies. Panel (a) shows the internal energy map in the θ_1-$\Delta\theta$ coordinates. (b), (c) Gibbs energy G of the same sample in the same phase space at $k_BT = 0.2K$ and $k_BT = 0.35K$, respectively, with K the anisotropy constant (density of states $\rho = 100$). (d) Cross section of the maps (a)–(c) at $\Delta\theta = \pi/2$ and $\Delta\theta = 2\pi/3$. Cross-section line styles correspond to those in (a)–(c).

IV. ANALYTICAL CALCULATION OF THE FREE ENERGY

To study the influence of the finite temperature on these local energy minima the free energy landscape has been calculated analytically. The free energy can be calculated as

$$G = E - TS = E - k_BT \ln(\Omega_E), \tag{7}$$

where E is internal energy, k_B the Boltzmann constant, S the entropy, and Ω_E the number of states with energy E. The Ω_E is unity for each of collinear states described in the previous paragraph. For noncollinear states the number of states corresponds to the length of a circle made by the first spin on the surface of a unity sphere: $\Omega_E = \int_0^{2\pi} \rho \cos(\theta_1) d\theta_1 = 2\pi\rho \sin(\theta_1)$, where ρ is the number of states per unit radian. Indeed, the first magnetic moment can have $2\pi\rho \sin(\theta_1)$ orientations, while orientations of other moments for a configuration of an energy E are fixed by the angle $\Delta\theta$ between them and the angle $\theta_1 + n\Delta\theta$ with respect to the z axis. Figures 4(b) and 4(c) give $G(\theta_1, \Delta\theta)$ for two different temperatures, while Fig. 4(d) shows the cross sections of the energy landscape of Figs. 4(a)–4(c) for vanishing J. The two solid lines in Fig. 4(d) correspond to the internal energy of Fig. 4(a). The straight solid line shows the band of saddle points at $\Delta\theta = \pi/2$, while the sine-shaped solid line corresponds to local energy minimum at $\Delta\theta = 2\pi/3$. The dashed and dotted lines correspond to the free energy for $\Delta\theta = 2\pi/3$ and $k_BT = 0.2K$ and $0.35K$, respectively. The density of states ρ influences the absolute value of the free energy but does not change either positions or shapes of minima and maxima. The total number of local energy minima is directly proportional to the number of sites in a chain. Particularly, the minima appear when $\Delta\theta = 2\pi m/(N-1)$ with integer $m \in [1, N-1]$. Therefore, there are nine local energy minima for the chain consisting of four effective magnetic moments, while their number increases to twelve for the chain of five moments, etc. Inclusion of the dipolar interaction enhances the anisotropy and, therefore, make the local energy minima deeper. Thus, the number of noncollinear configurations increases for longer chains.

Interestingly, the entropy changes the energy landscape significantly. Particularly, the entropy of the internal energy minima corresponding to noncollinear configurations is much larger than that of collinear states. As a consequence the local energy minima at $\theta_1 = 0$ split. The splitting increases with increasing temperature and corresponds to complicated noncollinear magnetic states. Hence, the local minima of the free energy in periodic chains might correspond to AFSS or KS and are very important in determination of magnetization configurations at finite temperatures. This effect is particularly important if the lifetime of a metastable state is comparable to or larger than the characteristic time of the measurement. Another interesting observation from Fig. 4 is that the local minima of the free energy correspond to the nonhomogeneous spin spiral; that is, in one part of the spiral the rotation happens quicker than in another. One can regard such configuration as almost collinear antiferromagnetic domains with knotlike solitons between those described above. Among other things this finding explains why one finds domain walls in antiferromagnetic systems, where the domain walls are energetically unfavorable.

V. MONTE CARLO SIMULATIONS

In realistic systems one has to consider three-dimensional Heisenberg spins as well as dipolar interactions. This makes the phase space very complicated and inaccessible by analytical calculations. To check the stability of described metastable solutions we have performed extended Monte Carlo (MC) simulations of finite magnetic chains of different lengths. Particular attention has been paid to the closed rings consisting of effective magnetic moments coupled by dipolar and antiferromagnetic exchange interactions as well as subject to the on-site uniaxial anisotropy, because in this case an additional aspect of spin parity becomes important.

To study the magnetic states of these structures we carried out MC simulations with the Metropolis algorithm under local dynamics and the single spin flip method [23]. Technical aspects of the MC procedure can be found in [23,24]. The energy is given in Eq. (1). Since we consider an antiferromagnetic coupling between neighboring sites J values between -0.1 and -40 meV have been explored. This range of values includes systems reported by Savina *et al.* [25] and references therein. The simulations have been started with a random orientation of magnetic moments. The new orientation of each randomly chosen magnetic moment has been accepted

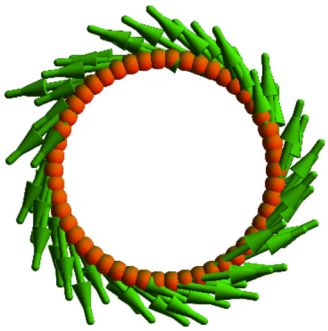

FIG. 5. Equilibrium MC configuration of a chain consisting of 50 moments for $D = 1$, and $J = 0$ meV and $K = 0$ meV.

with a Boltzmann probability $p = \min(1, \exp(-\Delta E/k_B T))$. The rings were relaxed using a tempered annealing procedure until the equilibrium configuration has been achieved. Relatively low finite temperatures $k_B T \ll |J|$ have been used in the calculations. The number of Monte Carlo steps (MCS) considered in each relaxation process was 3×10^7. To distinguish between effects induced by different energy contributions we start looking for equilibrium states of the system considering involved energies separately. After that we explore the differences that appear due to variation of the anisotropy and the number of elements in the ring.

To analyze the impact of the different variables we start by looking to the purely dipolar case, that is, $J = K = 0$. In this case, independently of the number of sites in the ring, the magnetic configuration at remanence is a closured-vortex-like state, as illustrated in Fig. 5. For $J = 0$ and $D = 0$ two cases can be distinguished: easy z axis for $K > 0$ and easy xy plane for $K < 0$. For $K = 0.1$ meV, magnetic moments align themselves parallel to the z axis, while the orientation of each moment (up or down) is random, as shown in Fig. 6(a). When $K = -0.1$ meV, the ring exhibits an in-plane magnetization. Similarly to the previous case the orientation of each moment in the plane is random, as evidenced in Fig. 6(b). In the purely antiferromagnetic case, that is $K = 0$ and $D = 0$, differences appear when considering rings with odd and even numbers of sites,

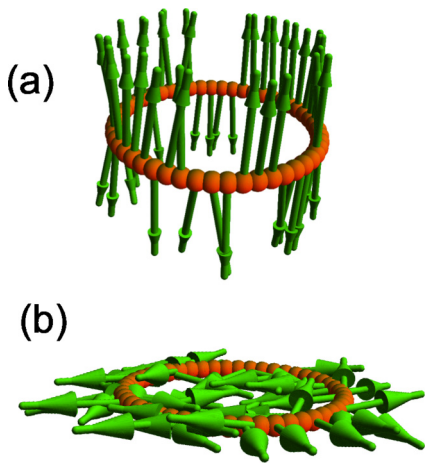

FIG. 6. Equilibrium MC configuration of a chain consisting of 50 moments for $D = 0$, $J = 0$ meV and (a) $K = 0.4$ meV and (b) $K = -0.4$ meV.

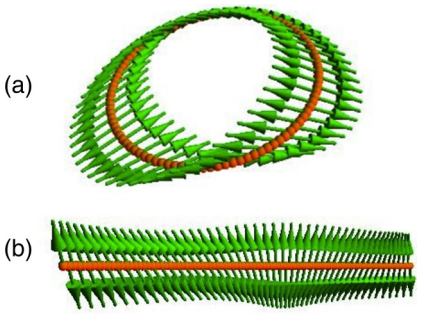

FIG. 7. Equilibrium MC configuration of a chain consisting of 100 moments for $D = 0$, $K = 0$ meV, $J = -40$ meV: (a) closed AFM configuration and (b) the same shown with open ends for clarity.

for example $N = 100$ and $N = 101$. For even N and with no anisotropy and dipolar interaction involved a perfect antiferromagnetic ordering has been found as shown in Fig. 7(a). When we include an additional particle, $N = 101$, a knot soliton appears due to geometrical frustration, as shown in Fig. 8(a). Hence, the local energy minima described in Fig. 4 do not survive in the Monte Carlo simulations, because their lifetimes are too short and the energy barriers can be easily overcome.

Once the role of every contribution to the energy has been analyzed separately, we consider all of them together, that is, $D = 1$, $J = -40$ meV, and $K = \pm 0.4$ meV. For the sake of generality the chain length has been varied between 10 and 110 sites. Very short chains do not show any particularly surprising results. One finds a perfect AFM alignment for even N, while Möbius configurations for odd N. Depending on the direction of the easy axis two different orientations of KS can be found as shown in Figs. 8 and 9. These two different types of KS are labeled KN and KB due to the similarity they showed to Néel (see Fig. 8) and Bloch walls (see Fig. 9), respectively. For $K = 0$, both types of configurations KB and KN can be observed. The longer chains with anisotropy, however, show AFSS as equilibrium states for even N.

We also observe a relation between number of knots, number of sites, and anisotropy. For an odd number of sites all rings exhibit knots due to geometrical frustration. Most interestingly, however, we find the Möbius-like structure also in antiferromagnetic rings with an even number of effective moments. When considering an even number of sites, larger values of K are needed to observe knots at a lower number of sites. For example, for vanishing K, 100 sites are needed in the ring to observe a first knot,

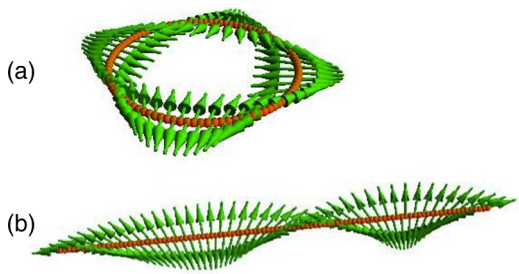

FIG. 8. Equilibrium MC configuration of a chain consisting of 100 moments for $D = 1$, $K = -0.4$ meV, $J = -40$ meV: (a) closed KN configuration and (b) the same shown with open ends for clarity.

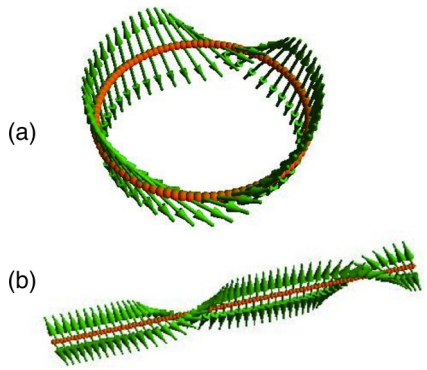

FIG. 9. Equilibrium MC configuration of a chain consisting of 100 moments for $D = 1$, $K = 0.4$ meV, $J = -40$ meV: (a) closed KB configuration and (b) the same shown with open ends for clarity.

while 80 sites are needed if $K = \pm 0.01J$, and 40 sites are needed for $K = \pm 0.1J$. This means that the local energy minimum becomes significantly populated only at large N. MC simulations have been designed to find the statistical averages by exploring the energy landscape. So, ideally at the end of the simulation the averaging over the infinitely long time should result in the exact expectation values for the observables. At low temperatures and for large systems, however, the time scale of simulations is much smaller than the correlation times as we have shown recently [26]. For the reason of insufficient averaging and long lifetimes of the excited states the deepest local minima with the lowest number of knots can be observed in the MC simulations. A typical MC relaxation of a KB state is shown in Fig. 10. Monte Carlo steps do not correspond to real time steps and, hence, do not provide us with reliable information on the nonequilibrium dynamics or the real relaxation time. However, it is important to note that the lifetimes of the metastable noncollinear states described in this paper might be finite and, hence, lowest KB or KN configurations might be detected experimentally. The investigation of the nonequilibrium dynamics of these metastable spin helices, therefore, would be of great interest. Because the strong anisotropy makes the local minima deeper, the noncollinear states are more easily found for higher

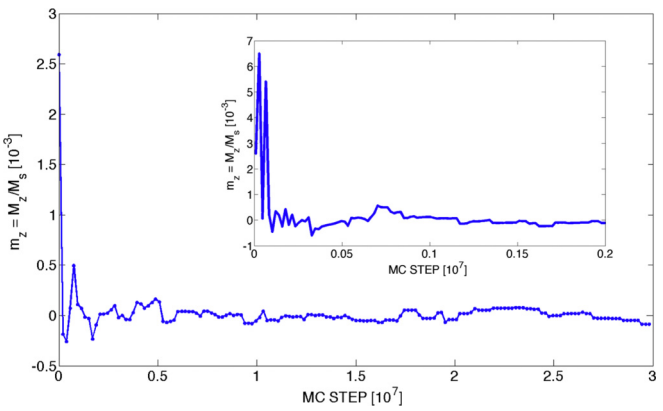

FIG. 10. Typical MC relaxation of a chain consisting of 50 moments with $D = 1$, $K = 0.4$ meV, $J = -40$ meV at $T = 0.0001$ K. The inset shows the fast part of the relaxation process. In this case, the magnetic configuration corresponds to KB configuration.

anisotropy values. This nicely corresponds to the analytical considerations made above.

VI. CONCLUSIONS

To conclude, in this paper we show analytically that closed chains coupled by antiferromagnetic exchange and subject to perpendicular magnetic anisotropy possess local energy minima corresponding to noncollinear topological spin spirals. Analytical analysis of the free energy at finite temperatures for chains with dominating anisotropy has shown that anisotropy increases the depth of the local energy minima. This makes the noncollinear configurations particularly stable for such chains ($|K| \gg |J|$). The large depth of the local energy minima results, in turn, in the increase of the activation energy needed for the relaxation towards the global energy minimum (collinear antiferromagnetic configuration). As the lifetimes of magnetic configurations exponentially depend on the activation energy ΔE ($\tau \propto \exp[\Delta E / k_B T]$) the lifetimes of the noncollinear configurations strongly increase with increasing anisotropy and decreasing temperature. Another important effect concerned with magnetic anisotropy is that with increasing anisotropy the extended spin spirals become energetically less favorable than localized kink solitons. Depending on the sign of the anisotropy constant two configurations for the kink soliton are possible: for $K > 0$, a Bloch-like KB soliton is stabilized, while for $K < 0$ a Néel-like KN soliton appears. A similar effect is observed when the dipolar interaction is introduced into the Hamiltonian: first, the dipolar interaction make the local minima deeper because it induces magnetic anisotropy and, second, it might lead to transformation of the spin spirals to kink solitons.

The number of the local energy minima increases with the number of magnetic moments, because the angle between neighboring magnetic moments for configuration corresponding to an energy minimum in a spiral equals $\Delta\theta = 2\pi m/(N - 1)$. In a kink soliton this relation is more complicated but the tendency is similar. Therefore, increase of the chain's length and the anisotropy leads to a complicated energy landscape with multiple local energy minima. Some of these minima are very deep and the lifetimes of corresponding states are large. For that reason the deepest local energy minima become populated also in the Monte Carlo simulations in long closed structures. Particularly interesting is the Möbius antiferromagnetic configurations with an even number of sites in closed chains. While the existence of such a configuration in chains with an odd site number has been reported, a similar configuration in chains with an even number of sites was unknown up to now. The noncollinear states can be found in closed geometry of any shape. Although both methods, analytical calculations and numerical simulations, have been performed independently, they lead to consistent results and allowed us to validate the conclusions from different points of view.

Eventually, we would like to discuss the results presented above in view of experiments. First of all, obtained data allow us to explain several existing experiments. Particularly, there are several reports on experimental observation of antiferromagnetic domain walls—for example in Fe monolayers on W(001) [27] or in antiferromagnetic chains on the basis of superlattices [28] despite the fact that the ground state for

both systems is known to be a collinear antiferromagnetic configuration. The existence of antiferromagnetic domain walls has always been attributed to pinning, to defects, or to very rapid relaxation of a system. However, the reason why a rapid relaxation should lead to the domain walls and not to another trapped configuration has never been clarified. Our results demonstrate that indeed an abrupt cooling of an antiferromagnetic system should lead to formation of kink solitons which are mathematically equivalent to the domain walls. Additionally, our investigation calls for reinvestigation of some experimental results. Particularly, the magnetic configuration in antiferromagnetic chains found experimentally in [2] has limited agreement with theoretically predicted ground states at low fields. One possible reason could be that the measured configurations are not the ground states but rather the antiferromagnetic metastable spin spirals with long lifetimes predicted in the present paper. Hence, our investigation brings light onto the known results and might explain existing experimental data.

ACKNOWLEDGMENTS

E.Y.V. and M.K. acknowledges support by the Collaborative Project of DFG SFB668. In Chile we acknowledge support from Fondecyt Grant No. 1160198 and Financiamiento Basal para Centros Científicos y Tecnológicos de Excelencia FB0807. S.C.-S. also acknowledges support from a Conicyt fellowship for doctoral studies.

APPENDIX: DETAILS OF CALCULATIONS

1. Energy of an antiferromagnetic spin spiral

Let us consider a chain with N magnetic moments coupled by a nearest-neighbor antiferromagnetic exchange interaction, which are in a spiral configuration. In this case the spatial dependence of magnetization can be described as

$$\vec{S}\left(i,\Delta\theta_k^{(N)}\right)=\vec{S}_x\left(i,\Delta\theta_k^{(N)}\right)+\vec{S}_z\left(i,\Delta\theta_k^{(N)}\right), \tag{A1}$$

$$\vec{S}_z\left(i,\Delta\theta_k^{(N)}\right)=\cos\left[(i-1)\Delta\theta_k^{(N)}\right]\hat{z},$$
$$\vec{S}_x\left(i,\Delta\theta_k^{(N)}\right)=\sin\left[(i-1)\Delta\theta_k^{(N)}\right]\hat{x}. \tag{A2}$$

To have a ring with periodic boundary conditions $\vec{S}(1,\Delta\theta_k^{(N)})=\vec{S}(N+1,\Delta\theta_k^{(N)})$, it is necessary that $N\Delta\theta_k^{(N)}=2\pi k$, with k an integer value between 1 and $N-1$. If $N=2P$, then $\Delta\theta=\pi k/P$. On the other hand, since k can take values between 1 and $N-1$, there is a stable antiferromagnetic configuration. When $N=2P+1$, $2k$ will be always an even number and smaller than N; i.e., it is not possible to obtain π. Therefore the antiferromagnetic configuration is forbidden. Let us see this situation in terms of the energy of the system:

$$E\left(\Delta\theta_k^{(N)}\right)=\mathcal{J}\sum_{i=1}^{N}\vec{S}\left(i,\Delta\theta_k^{(N)}\right)\cdot\vec{S}\left(i+1,\Delta\theta_k^{(N)}\right)-K\sum_{i=1}^{N}S_z^2 \tag{A3}$$

$$=\mathcal{J}N\cos\left(\Delta\theta_k^{(N)}\right)-K\sum_{i=1}^{N}\cos^2\left[(i-1)\Delta\theta_k^{(N)}\right], \tag{A4}$$

with $J=-\mathcal{J}$. Minimizing the previous equation, we have

$$\frac{dE}{d\Delta\theta_k^{(N)}}\left(\Delta\theta_k^{(N)}\right)=-\mathcal{J}N\sin\left(\Delta\theta_k^{(N)}\right)+2K\sum_{i=1}^{N}(i-1)\cos\left[(i-1)\Delta\theta_k^{(N)}\right]\times\sin\left[(i-1)\Delta\theta_k^{(N)}\right]=0. \tag{A5}$$

When N is even, the solution is $\Delta\theta_{N/2}^{(N)}$, but when N is an odd number, the system has two solutions that satisfy the minimum energy condition $\Delta\theta_{(N/2)\pm(1/2)}^{(N)}$. This is equivalent to the existence of an antiferromagnetic state for N even, i.e.,

$$N\Delta\theta_{N/2}^{(N)}=\pi N\Rightarrow\Delta\theta_{N/2}^{N}=\pi, \tag{A6}$$

with energy given by

$$E=-\mathcal{J}N-KN=-N(\mathcal{J}+K). \tag{A7}$$

When N is odd, $\Delta\theta_{(N/2)\pm(1/2)}^{(N)}$, then in the minimum energy state we have

$$N\Delta\theta_{(N/2)\pm(1/2)}^{(N)}=\pi(N\pm1)\Rightarrow\Delta\theta_{N/2}^{N}=\pi\pm\frac{\pi}{N}, \tag{A8}$$

and its energy is

$$E=-\mathcal{J}N\cos(\pi/N)-K\sum_{i=1}^{N}\cos^2[(i-1)\pi/N]. \tag{A9}$$

Figure 1 of the main text illustrates the energy for different N values.

2. Energy of antiferromagnetic domains separated by a spin spiral

Let us consider a system with N magnetic moments, where M magnetic moments form the helical configuration, and $N-M$ magnetic moments are in an antiferromagnetic state. In this case we have

$$E=E\left(\mathrm{AFM}_M^N\right)+E\left(\Delta\theta_k^{(M)}\right). \tag{A10}$$

a. N even and M odd

In this case, $N-M$ is an even number; therefore, if the first magnetic moment of the AFM region is $\downarrow$, then the last magnetic moment will be $\uparrow$. The energy of this AFM region is

$$E\left(\mathrm{AF}_M^N\right)=-\mathcal{J}(N-M-1)-K(N-M). \tag{A11}$$

Now, if we have a spiral state with the first magnetic moment pointing $\uparrow$, which, because of the boundary conditions, is also the last magnetic moment of the AF state, the energy of this state is

$$E\left(\Delta\theta_k^{(M)}\right)=\mathcal{J}M\cos\left(\Delta\theta_k^{(M)}\right)-K\sum_{i=1}^{M}\cos^2\left[(i-1)\Delta\theta_k^{(M)}\right], \tag{A12}$$

with $M\Delta\theta_k^{(M)}=2\pi k$. Finally, the interaction between the first magnetic moment of the spiral configuration and the first

magnetic moment of the AFM configuration is $-\mathcal{J}$, so the energy is

$$E = -\mathcal{J}(N-M) - K(N-M) - \mathcal{J}M\cos\left(\Delta\theta_k^{(M)}\right) - K\sum_{i=1}^{M}\cos^2\left[(i-1)\Delta\theta_k^{(M)}\right]. \quad \text{(A13)}$$

Then $\Delta\theta_k^{(M)}$ minimizes Eq. (A13) for $k = M/2$, i.e., if $\Delta\theta_{M/2}^{(M)} = \pi$. Therefore, the energy of this spiral configuration will be the same as the full AFM state [see Eq. (A7)], i.e.,

$$E = -N(\mathcal{J}+K). \quad \text{(A14)}$$

b. N even and M odd

In this case $N-M$ is odd, so if the first magnetic moment of the AFM region is $\downarrow$, then the last one will be $\downarrow$. For this case, the energy of the region is

$$E\left(\mathrm{AFM}_M^N\right) = -\mathcal{J}(N-M-1) - K(N-M). \quad \text{(A15)}$$

Now, we can consider the spiral state whose formation starts with a magnetic moment pointing $\uparrow$, and satisfies that this magnetic moment is also the last magnetic moment in the AFM state. The energy obtained in this case is given by

$$E\left(\Delta\theta_k^{(M)}\right) = \mathcal{J}M\cos\left(\Delta\theta_k^{(M)}\right) - K\sum_{i=1}^{M}\cos^2\left[(i-1)\Delta\theta_k^{(M)}\right], \quad \text{(A16)}$$

with $M\bar{\Delta\theta}_k^{(M)} = 2\pi k - \pi$. Finally, the interaction between the first magnetic moment of the spiral configuration and the first magnetic moment of the AFM configuration is given by $-\mathcal{J}$, so the energy expression is

$$E = -\mathcal{J}(N-M) - K(N-M) - \mathcal{J}M\cos\left(\bar{\Delta\theta}_k^{(M)}\right) - K\sum_{i=1}^{M}\cos^2\left[(i-1)\bar{\Delta\theta}_k^{(M)}\right]. \quad \text{(A17)}$$

We minimize this term when $\bar{\Delta\theta}_k^{(M)} = \pi$, and then we obtain the AFM state again.

c. N odd and M odd

In this case $N-M$ is even. In this way, if the first magnetic moment of the AFM semistate is pointing $\downarrow$, then the last moment will be pointing $\uparrow$. Therefore, the energy of this semistate is given by

$$E\left(\mathrm{AFM}_M^N\right) = -\mathcal{J}(N-M-1) - K(N-M). \quad \text{(A18)}$$

Let us consider now the spiral region that starts with a magnetic moment pointing $\uparrow$. This moment is the same as the last moment of the AFM region. Under this consideration, the energy of this state is

$$E = -\mathcal{J}M\cos(\pi/M) - K\sum_{i=1}^{M}\cos^2[(i-1)\pi/M]. \quad \text{(A19)}$$

The total energy is

$$E\left(\mathrm{AFM}_M^N\right) = -\mathcal{J}(N-M) - K(N-M) - \mathcal{J}M\cos(\pi/M) - K\sum_{i=1}^{M}\cos^2[(i-1)\pi/M]. \quad \text{(A20)}$$

If we compare this energy with the full AFM configuration energy for a ring with an odd number of elements N, we have

$$\Delta E = -\mathcal{J}N\cos(\pi/N) - K\sum_{i=1}^{N}\cos^2[(i-1)\pi/N] + \mathcal{J}(N-M) + K(N-M) + \mathcal{J}M\cos(\pi/M) + K\sum_{i=1}^{M}\cos^2[(i-1)\pi/M], \quad \text{(A21)}$$

$$\Delta E = \mathcal{J}\{N[1-\cos(\pi/N)] - M[1-\cos(\pi/M)]\} - K\left\{\sum_{i=1}^{N}\cos^2[(i-1)\pi/N] - \sum_{i=1}^{M}\cos^2[(i-1)\pi/M]\right\} + K(N-M). \quad \text{(A22)}$$

If $\Delta E > 0$, then the second configuration minimizes the energy. If we consider the function

$$\mathcal{K}(x) = \mathcal{J}x[1-\cos(\pi/x)] - K\sum_{i=1}^{x}\cos^2[(i-1)\pi/x] + Kx, \quad \text{(A23)}$$

then

$$\Delta E = \mathcal{K}(N) - \mathcal{K}(M). \quad \text{(A24)}$$

Figure 3(a) of the main text shows the behavior of ΔE for $J = 1$ meV and $N = 31$. There is no change in the behavior of M as a function of K for any N. This is shown in Fig. 3(b) of the main text.

[1] E. Y. Vedmedenko and D. Altwein, Phys. Rev. Lett. **112**, 017206 (2014).

[2] A. A. Khajetoorians, J. Wiebe, B. Chilian, S. Lounis, S. Blügel, and R. Wiesendanger, Nat. Phys. **8**, 497 (2012).

[3] Y. T. Millev, E. Vedmedenko, and H. P. Oepen, J. Phys. D: Appl. Phys. **36**, 2945 (2003).

[4] R. Skomski, Z. Li, Rui Zhang, R. D. Kirby, A. Enders, D. Schmidt, T. Hofmann, E. Schubert, and D. J. Sellmyer, J. Appl. Phys. **111**, 07E116 (2012).

[5] L. Trallori, P. Politi, A. Rettori, M. G. Pini, and J. Villain, Phys. Rev. Lett. **72**, 1925 (1994).

[6] A. P. Popov, A. V. Anisimov, O. Eriksson, and N. V. Skorodumova, Phys. Rev. B **81**, 054440 (2010).

[7] L. V. Dzemiantsova, G. Meier, and R. Röhlsberger, Sci. Rep. **5**, 16153 (2015).

[8] A. P. Popov, A. Rettori, and M. G. Pini, Phys. Rev. B **92**, 024414 (2015).

[9] S. Boso, Contemp. Phys. **48**, 13 (2007).
[10] L. Zhou, J. Wiebe, S. Lounis, E. Y. Vedmedenko, F. Meier, S. Blügel, P. H. Dederichs, and R. Wiesendanger, Nat. Phys. **6**, 187 (2010).
[11] M. Haque, V. R. Chandra, and J. N. Bandyopadhyay, Phys. Rev. A **79**, 042317 (2009).
[12] J. R. Friedman, M. P. Sarachik, J. Tejada, and R. Ziolo, Phys. Rev. Lett. **76**, 3830 (1996).
[13] B. Behin-Aein, D. Datta, S. Salahuddin, and S. Datta, Nat. Nanotechnol. **5**, 266 (2010).
[14] J. P. Morgan, A. Stein, S. Langridge, and C. H. Marrows, Nat. Phys. **7**, 75 (2011).
[15] A. Schumann, P. Szary, E. Y. Vedmedenko, and H. Zabel, New J. Phys. **14**, 035015 (2012).
[16] O. Cador, D. Gatteschi, R. Sessoli, A.-L. Barra, G. A. Timcoc, and R. E. P. Winpenny, J. Magn. Magn. Mater. **290-291**, 55 (2005).
[17] K. Bernot, L. Bogani, A. Caneschi, D. Gatteschi, and R. Sessoli, J. Am. Chem. Soc. **128**, 7947 (2006).
[18] W. Wernsdorfer, Nat. Mater. **6**, 174 (2007).
[19] A. Fernández-Pacheco, D. Petit, R. Mansell, R. Lavrijsen, J. H. Lee, and R. P. Cowburn, Phys. Rev. B **86**, 104422 (2012).
[20] D. Petit, R. Lavrijsen, J. H. Lee, R. Mansell, A. Fernández-Pacheco, and R. P. Cowburn, Nanotechnology **27**, 155203 (2016).
[21] R. Lavrijsen, J. H. Lee, A. Fernández-Pacheco, D. C. M. C. Petit, R. Mansell, and R. P. Cowburn, Nature (London) **493**, 647 (2013).
[22] L. M. Sandratskii, J. Phys.: Condens. Matter **3**, 8565 (1991).
[23] K. Binder and D. W. Heerman, *Monte Carlo Simulation in Statistical Physics* (Springer, New York, 2002).
[24] E. Y. Vedmedenko, Phys. Status Solidi B **244**, 1133 (2007).
[25] Y. Savina, O. Bludov, V. Pashchenko, S. L. Gnatchenko, P. Lemmens, and H. Berger, Phys. Rev. B **84**, 104447 (2011).
[26] E. Y. Vedmedenko, N. Mikuszeit, T. Stapelfeldt, R. Wieser, M. Potthoff, A. I. Lichtenstein, and R. Wiesendanger, Eur. Phys. J. B **80**, 331 (2011).
[27] M. Bode, E. Y. Vedmedenko, K. von Bergmann, A. Kubetzka, P. Ferriani, S. Heinze, and R. Wiesendanger, Nat. Mater. **5**, 477 (2006).
[28] A. Fernández-Pacheco, R. Mansell, J. Lee *et al.*, in *Topological Structures in Ferroic Materials: Domain Walls, Vortices and Skyrmions*, edited by J. Seidel, Springer Series in Materials Science Vol. 228 (Springer International Publishing, New York, 2016), pp. 219–238.